Cellular and Molecular Life Sciences (2025) 82:92
https://doi.org/10.1007/s00018-025-05591-2

ORIGINAL ARTICLE

Male germ cells with *Bag5* deficiency show reduced spermiogenesis and exchange of basic nuclear proteins

Yuming Cao[1] · Shengnan Wang[1] · Zihan Qin[2,3] · Qiaohua Xiong[2,3] · Jie Liu[1] · Wenwen Li[1] · Liyang Li[1] · Fei Ao[1] · Zexiao Wei[1] · Li Wang[1]

Received: 25 April 2024 / Revised: 8 January 2025 / Accepted: 12 January 2025

Abstract

Bcl-2 associated athanogene-5 (BAG5) represents a unique BAG cochaperone family member, regulating chaperone activity. We first demonstrated significant differences in *Bag5* expression by RNA seq analysis of teratozoospermia and healthy male sperm samples, but the genetic and molecular mechanisms governing this process remain elusive. We further found that BAG5 has highest expression in human and mouse testes. BAG5 expression is elevated in late stage pachytene spermatocytes and spermatids. Targeted *Bag5* inactivation in mice induces massive apoptosis in male germ cells and abrogates male infertility. The ordered loading of sperm basic nuclear proteins on chromatin is altered, with lost TNPs and PRMs, resulting in severe sperm head deformity and partial 9 + 2 microtubule structure disorder. In terms of mechanism, immunoprecipitation (IP)-mass spectroscopy (MS) revealed BAG5 interacts with HSPA2, a testis-specific HSP70 family member regulating the transcription of the transition protein TNPs as well as spermatogenesis. RNA-sequencing assessment of *Bag5* deficient testis confirmed *Bag5* participation in transcriptional repression and revealed significant changes in *Hspa2* expression. *Bag5* deficiency resulted in decreased levels of HSPA2, germ cell apoptosis and subsequent inappropriate nuclear protein deposition and chromatin condensation. Decreased BAG5 expression levels in patients with non-obstructive azoospermia and oligoasthenospermia were also detected. These results uncovered an intriguing HSPA2-mediated key function of BAG5, which may constitute a potential prognostic biomarker of male infertility.

Keywords BAG5 · Infertility · Sperm head deformity · Inappropriate nuclear protein deposition

Introduction

Spermatogenesis involves complex events in male reproduction, with diploid spermatogonia successively undergoing mitosis, meiosis and spermiogenesis to produce haploid spermatozoa [1]. Spermiogenesis in mammalians requires substantial morphological alterations and intense regulation of specific genes, which jointly induce structural remodeling of sperm chromatin [2, 3]. Chromatin remodeling represents a critical epigenetic process in the development of germs, facilitating condensation, protecting paternal genome, promoting sperm maturation and ensuring fertility [4]. In this process, a great amount of core histones are first hyperacetylated and subsequently replaced by transition proteins that are then also substituted by protamines [5, 6]. Although histone-to-protamine transition is crucial in spermatogenesis, how it is affected remains completely undefined.

In spermiogenesis, round spermatids undergo multiple critical alterations such as elongation and nuclear condensation [7, 8]. Histones after acetylation are substituted by transition proteins (TNP1 and TNP2) and then by PRM1 and PRM2, which orchestrate the packaging of sperm genome into a different toroid chromatin structure [9, 10]. Both TNPs and PRMs contribute to chromatin remodeling and DNA condensation in which 85 to 95% of sperm histones are substituted by PRMs [11, 12]. Chromatin remodeling

✉ Li Wang
wangli223@mail.sysu.edu.cn

1 Department of Obstetrics and Gynecology, Perinatal Medical Center, The Fifth Affiliated Hospital of Sun Yat-Sen University, No. 52 Meihua East Road, Zhuhai, Guangdong, People's Republic of China

2 Reproductive Medicine Center, Zhongnan Hospital of Wuhan University, Wuhan, People's Republic of China

3 Hubei Clinical Research Center for Prenatal Diagnosis and Birth Health, Wuhan 430071, Hubei, People's Republic of China

Published online: 24 February 2025

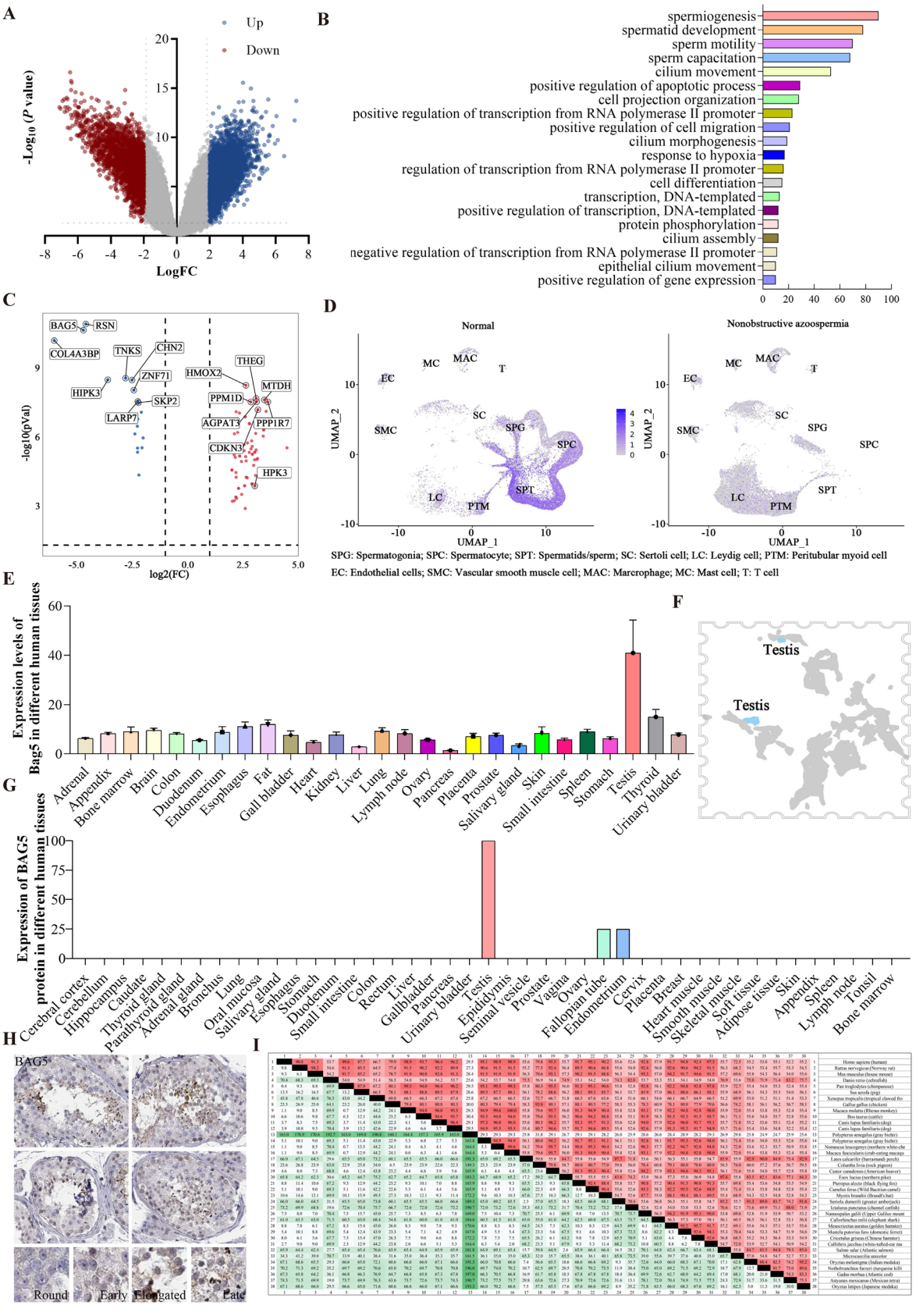
A
Up
Down
-Log10 (P value)
LogFC
B
spermiogenesis
spermatid development
sperm motility
sperm capacitation
cilium movement
positive regulation of apoptotic process
cell projection organization
positive regulation of transcription from RNA polymerase II promoter
positive regulation of cell migration
cilium morphogenesis
response to hypoxia
regulation of transcription from RNA polymerase II promoter
cell differentiation
transcription, DNA-templated
positive regulation of transcription, DNA-templated
protein phosphorylation
cilium assembly
negative regulation of transcription from RNA polymerase II promoter
epithelial cilium movement
positive regulation of gene expression
C
BAG5
RSN
COL4A3BP
TNKS
CHN2
ZNF71
HIPK3
SKP2
LARP7
HMOX2
THEG
MTDH
PPM1D
AGPAT3
PPP1R7
CDKN3
HPK3
-log10(pVal)
log2(FC)
D
Normal
Nonobstructive azoospermia
UMAP_1
UMAP_2
EC
MC
MAC
T
SMC
SC
SPG
SPC
SPT
LC
PTM
SPG: Spermatogonia; SPC: Spermatocyte; SPT: Spermatids/sperm; SC: Sertoli cell; LC: Leydig cell; PTM: Peritubular myoid cell
EC: Endothelial cells; SMC: Vascular smooth muscle cell; MAC: Marcrophage; MC: Mast cell; T: T cell
E
Expression levels of Bag5 in different human tissues
Adrenal
Appendix
Bone marrow
Brain
Colon
Duodenum
Endometrium
Esophagus
Fat
Gall bladder
Heart
Kidney
Liver
Lung
Lymph node
Ovary
Pancreas
Placenta
Prostate
Salivary gland
Skin
Small intestine
Spleen
Stomach
Testis
Thyroid
Urinary bladder
F
Testis
Testis
G
Expression of BAG5 protein in different human tissues
Cerebral cortex
Cerebellum
Hippocampus
Caudate
Thyroid gland
Parathyroid gland
Adrenal gland
Bronchus
Lung
Oral mucosa
Salivary gland
Esophagus
Stomach
Duodenum
Small intestine
Colon
Rectum
Liver
Gallbladder
Pancreas
Urinary bladder
Testis
Epididymis
Seminal vesicle
Prostate
Vagina
Ovary
Fallopian tube
Endometrium
Cervix
Placenta
Breast
Heart muscle
Smooth muscle
Skeletal muscle
Soft tissue
Adipose tissue
Skin
Appendix
Spleen
Lymph node
Tonsil
Bone marrow
H
BAG5
Round
Early Elongated
Late
I

◂**Fig. 1** Identification of *Bag5* as a key regulator of spermatogenesis. **A** RNA-seq datasets of 21 tissues from GEOdata were reanalyzed, comparison of gene expression between health and teratozoospermic man. Blue dots indicate upregulation, and red dots indicate downregulation. **B** The top GO terms associated with biological process, cellular component, and molecular function of differently expressed genes are shown. **C** Volcanic map annotation top 16 genes that are differentially expressed between health and teratozoospermic man. **D** MHA database analysis of *Bag5* expression in nonobstructive azoospermia and healthy male testicular tissue. **E**. NCBI database analysis *Bag5* mRNA expression in different human tissues. **F**, **G** The human protein atlas database analyzed the expression of BAG5 in different human tissues. **H** The human protein atlas database analyzed the localization of BAG5 in human testicular tissue. **I** Conservation analysis of BAG5 in different species

takes place after meiosis, with nucleosomal histones initially substituted by transition nuclear proteins and then by protamines for substantial chromatin compaction [13]. Any disruption in the sequence of TNPs or PRMs actions may impair sperm chromatin condensation, enhance oxidative stress, induce DNA strand breaks, and ultimately cause azoospermia because of induced apoptosis [14, 15]. Many genes that mediate germ cell apoptosis have a role in spermiogenesis [16, 17].

The BAG protein family comprises six different genetic products sharing one BAG domain that binds to the molecular chaperone HSP70 [18]. BAG5 is the only member with 5 BAG domains that cover the entire protein [19]. BAG proteins are known to control spermatozoa maturation and inhibit apoptosis [20]. BAG1 and BAG3 bind to BCL-2 to suppress apoptosis caused by many factors [21–23]. BAG4 binds to and blocks receptors of tumor necrosis factors [24]. BAG6 regulates the nuclear pathway communicating with mitochondria and controls cytochrome c release, thus regulating apoptosis [25]. As proapoptotic factors, BAGs act as nucleotide exchange factors of HSP70 to enhance protein refolding [26]. BAG2, BAG4 and BAG6 have been identified as key regulatory factors to stabilize germ cell development [27, 28]. However, the role of BAG5 is far from being elucidated.

Heat shock protein 70–2 (HSPA2), an abundantly expressed chaperone, promotes protein synthesis [29], translocation and folding [30]. HSPA2 contributes to fertility [31], affecting sperm quality and capacitation, sperm-egg recognition, and fertilization, which are crucial for reproduction in bulls [32]. HSPA2 also affects spermatogenesis, protecting cells from apoptosis and oxidative stress [33]. Fertilization success depends on both the number of spermatozoa detected in the female reproductive tract and the functional capability of these spermatozoa [34]. However, subfertility may be more related to altered molecular dynamics in spermatozoa that are undetectable by routine techniques. Therefore, molecular and omics assays were designed to assess critical aspects of molecular morphological features with high importance in sperm function.

Here, BAG5 was detected as an important modulator of spermatogenesis. *Bag5* knockout resulted in male infertility. Physiologically, *Bag5* deficiency substantially reduced sperm count and enhanced sperm abnormalities. Subsequent analysis revealed abnormal replacement of histone by protamine in $Bag5^{-/-}$ mice, with increased apoptotic germ cells. In terms of mechanism, immunoprecipitation (IP)-mass spectroscopy (MS) revealed an interaction between mouse BAG5 and HSPA2, which is required for transition protein transcription and spermatogenesis. Further evidence suggested that BAG5 expression was significantly decreased in both patients with nonobstructive azoospermia and oligoasthenospermia. Taken together, BAG5 as a critical regulator of HSPA2 affects multiple steps of spermatogenesis. These findings provide new insights into the role of protamine deposition during spermatogenesis.

Results

BAG5 is an important regulator of spermatogenesis

To identify candidate functional genes in spermatogenesis, we focused on the GEO database to re-analyze the current data. Based on a cross-platform microarray approach, the transcript profiles of sperm samples from 13 fertile men with ≥ 1 biological child and 8 men with teratozoospermia were examined. A volcano plot showed that 4118 and 2653 genes were upregulated and downregulated, respectively, in the teratozoospermia group versus fertile males (Fig. 1A). Cluster analysis showed that the most significantly affected genes were involved in spermiogenesis, followed by sperm motility, which also included genes related to the regulation of apoptosis (Fig. 1B). Further analysis of differential genes involved in spermatogenesis showed that 76 genes were up-regulated and 20 genes were down-regulated (Supplementary Table 3). We annotated and labeled the top 16 significantly regulated genes and found that *Bag5* expression was significantly reduced in patients with teratozoospermia (Fig. 1C). The MHA single cell database revealed significant differences in *BAG5* expression between different types of germ cells, especially spermatocytes and sperm

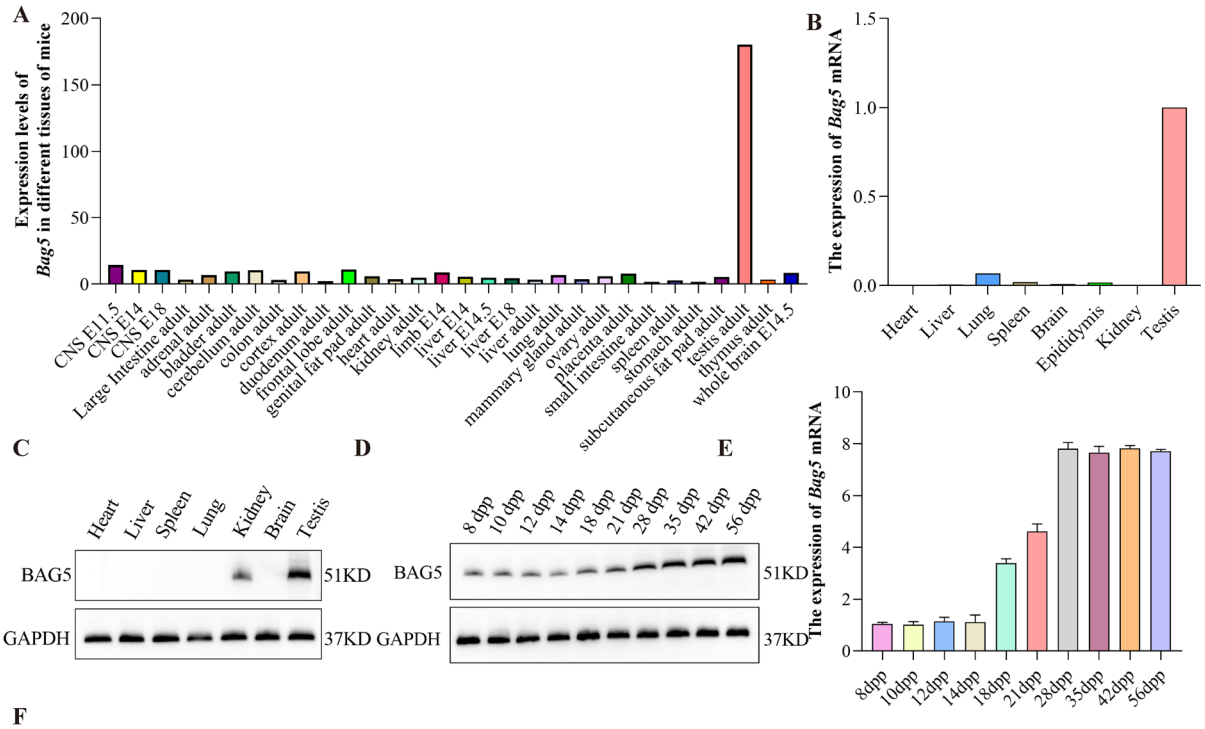
A
Expression levels of Bag5 in different tissues of mice
200
150
100
50
0
CNS E11.5
CNS E14
CNS E18
Large Intestine adult
adrenal adult
bladder adult
cerebellum adult
colon adult
cortex adult
duodenum adult
frontal lobe adult
genital fat pad adult
heart adult
kidney adult
limb E14
liver E14
liver E14.5
liver E18
liver adult
lung adult
mammary gland adult
ovary adult
placenta adult
small intestine adult
spleen adult
stomach adult
subcutaneous fat pad adult
testis adult
thymus adult
whole brain E14.5
B
The expression of Bag5 mRNA
1.5
1.0
0.5
0.0
Heart
Liver
Lung
Spleen
Brain
Epididymis
Kidney
Testis
C
Heart
Liver
Spleen
Lung
Kidney
Brain
Testis
BAG5
51KD
GAPDH
37KD
D
8 dpp
10 dpp
12 dpp
14 dpp
18 dpp
21 dpp
28 dpp
35 dpp
42 dpp
56 dpp
BAG5
51KD
GAPDH
37KD
E
The expression of Bag5 mRNA
10
8
6
4
2
0
8dpp
10dpp
12dpp
14dpp
18dpp
21dpp
28dpp
35dpp
42dpp
56dpp

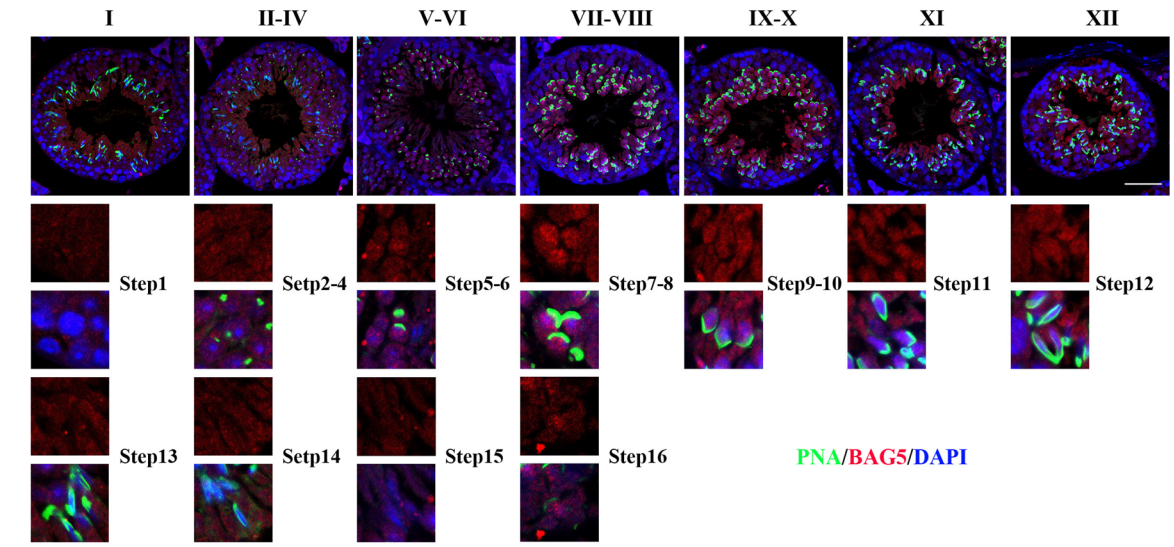
F
I
II-IV
V-VI
VII-VIII
IX-X
XI
XII
Step1
Setp2-4
Step5-6
Step7-8
Step9-10
Step11
Step12
Step13
Setp14
Step15
Step16
PNA/BAG5/DAPI

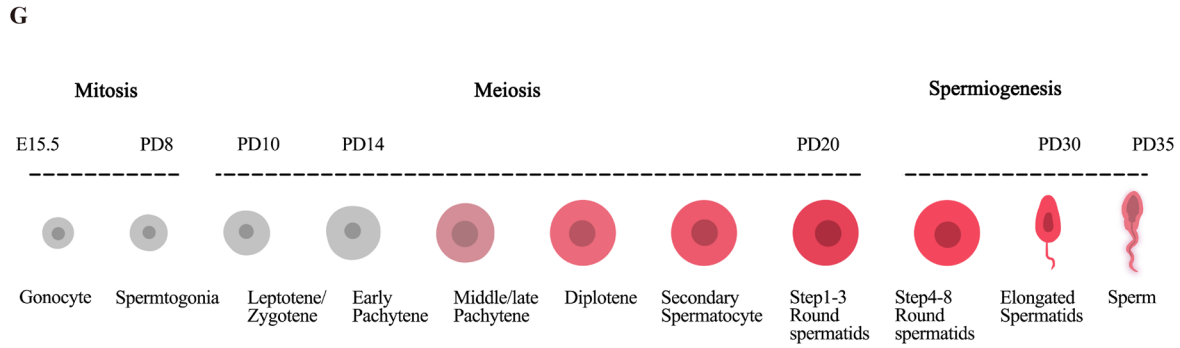
G
Mitosis
Meiosis
Spermiogenesis
E15.5
PD8
PD10
PD14
PD20
PD30
PD35
Gonocyte
Spermtogonia
Leptotene/ Zygotene
Early Pachytene
Middle/late Pachytene
Diplotene
Secondary Spermatocyte
Step1-3 Round spermatids
Step4-8 Round spermatids
Elongated Spermatids
Sperm

◂**Fig. 2** Expression and localization of BAG5 in mouse germ cells. **A** NCBI database analysis *Bag5* mRNA expression in different mice tissues. **B** The expression of *Bag5*mRNA in different tissues examined by RT-PCR. GAPDH loading as control. **C** The expression of BAG5 in different tissues examined by western blot. GAPDH loading as control. **D**, **E**. Expression of *Bag5* mRNA and protein in germ cells of mice at different developmental stages. **F** Localization of BAG5 in germ cells at different developmental stages in mice, scale bar, 50 μm. G. Pattern diagram of BAG5 expression and localization in germ cells

cells, between men with normal testis and non-obstructive azoospermia (http://malehealthatlas.cn/, Fig. 1D). The NCBI database identified the specific high expression profile of *BAG5* in the human testis (Fig. 1E). In addition, BAG5 expression at the protein level is consistent with mRNA amounts (https://www.proteinatlas.org/, Fig. 1F-G). The HUMAN PROTEIN ATLAS database showed that BAG5 is weakly expressed in spermatogonia, but more significantly expressed in elongated or late spermatids (Fig. 1H and Figure S1C). BAG5 is found in different species, with high homology (91.3%) between humans and mice. The above data pointed to BAG5 as an important regulator of male spermatogenesis that may play a consistent regulatory role across different species.

BAG5 expression is mostly detected in pachytene spermatocytes to late spermatogenesis in mice

We first examined *Bag5* mRNA and protein amounts in different mouse tissues, and found high levels in the adult testis (Fig. 2A–C). According to the MHA database, *Bag5* expression begins at mid-late pachytene spermatocytes and reaches a peak in spermatids (Figure S1A-B). In the first wave of murine spermatogenesis, late pachytene spermatocytes represent the most differentiated cells in seminiferous tubules in 18-day-old animals. *Bag5* mRNA and protein amounts rose from 14 to 18 dpp, reaching a peak at 28 dpp (Fig. 2D, E). Immunofluorescence analysis of testis samples from adult $Bag5^{+/+}$ mice detected *Bag5* in the nuclear and cytoplasmic compartments of spermatogenic cells, with protein amounts peaking in pachytene spermatocyte to elongate spermatocyte (Fig. 2F, G). These findings indicate BAG5 might regulate spermatocyte development or sperm deformation.

Bag5 knockout in testis results in decreased testis size, sperm count and fertility

To determine whether BAG5 plays a critical role in spermatogenesis, CRISPR-Cas9 was employed to disrupt *Bag5* gene (NCBI Reference Sequence: NM_027404; Ensembl: ENSMUSG00000049792) is located on mouse chromosome 12. Two exons are identified, with the ATG start codon in exon 2 and the TGA stop codon in exon 2 (Transcript: ENSMUST00000054636) (Fig. 3A). The target gene knockout positive 532 bp was identified by primer group 1, the target gene knockout negative 707 bp was identified by primer group 2, and both heterozygote mice showed positive. $Bag5^{-/-}$ mice, a product of intercrossed F1 $Bag5^{\pm}$ mice, had no BAG5 expression as detected by PCR and western blot, confirming successful knockout (Fig. 3B, C). $Bag5^{+/+}$ and $Bag5^{-/-}$ had similar body weights, but male $Bag5^{-/-}$ mice exhibited infertile during a 6-month continuous breeding (Fig. 3D). The overall appearance and weight of the testis were similar between $Bag5^{+/+}$ and $Bag5^{-/-}$ mice at 8 weeks old but these parameters decreased in $Bag5^{-/-}$ mice in comparison with $Bag5^{+/+}$ at 12 weeks of age (Fig. 3E, F). Hematoxylin/eosin staining revealed reduced germ cells and substantially decreased mature spermatozoa in the seminiferous tubules of $Bag5^{-/-}$ mice (Fig. 3G). At twelve weeks of age, our analysis revealed a significant decrease in both sperm quantity and motility in the caudal epididymis of $Bag5^{-/-}$ mice compared to their $Bag5^{+/+}$ counterparts (Fig. 3H-I). These results first demonstrated that BAG5 has an important function in spermatogenesis.

Deletion of *Bag5* leads to germ cell apoptosis

We first used STRA8, an initiation marker for germ cell entry into the meiotic process, to determine whether meiosis was initiated by germ cells. We randomly counted the seminiferous tubule in a section from 5 mice to count positive cells per tubule section. The results showed that fewer germ cells entered the meiotic process in the $Bag5^{-/-}$ group compared to $Bag5^{+/+}$ mice (Fig. 4A, B). Next, we examined the germ cell-specific marker DDX4, which was also detected in fewer germ cells in the $Bag5^{-/-}$ group compared to $Bag5^{+/+}$ mice (Fig. 4C, D). It is known BCL-2 suppresses apoptosis and is important for normal spermatogenesis. Meanwhile, BAG5 is also known as BCL2-associated athanogene protein. To investigate factors contributing to germ cell apoptosis in $Bag5^{-/-}$ mice, *Bcl-2* mRNA and protein amounts were assessed in mouse testis samples. The localization of

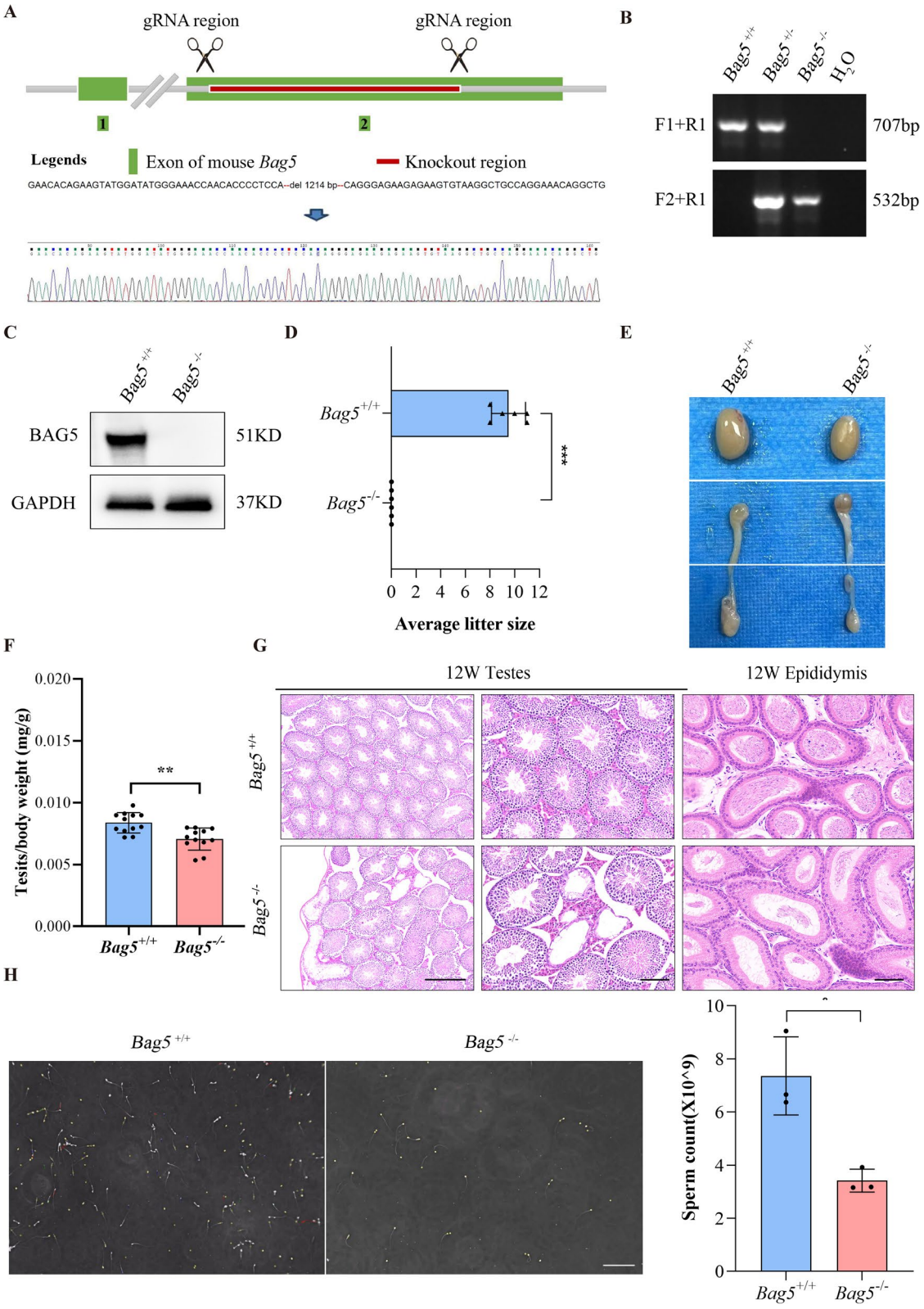
A
gRNA region
gRNA region
1
2
Legends
Exon of mouse Bag5
Knockout region
GAACACAGAAGTATGGATATGGGAAACCAACACCCCTCCA--del 1214 bp--CAGGGAGAAGAGAAGTGTAAGGCTGCCAGGAAACAGGCTG
B
Bag5+/+
Bag5+/-
Bag5-/-
H2O
F1+R1
707bp
F2+R1
532bp
C
Bag5+/+
Bag5-/-
BAG5
51KD
GAPDH
37KD
D
Bag5+/+
Bag5-/-
***
0 2 4 6 8 10 12
Average litter size
E
Bag5+/+
Bag5-/-
F
Tesits/body weight (mg/g)
0.020
0.015
0.010
0.005
0.000
**
Bag5+/+
Bag5-/-
G
12W Testes
12W Epididymis
Bag5+/+
Bag5-/-
H
Bag5+/+
Bag5-/-
Sperm count(X10^9)
10
8
6
4
2
0
Bag5+/+
Bag5-/-

◂**Fig. 3** Targeted disruption of *Bag5* caused infertility and abnormal spermatogenesis in mice. **A** Schematic representation of the recombination events targeting *Bag5* exon 2 using CRISPR/Cas9 technology. **B** The genotypes of wildtype, heterozygote and knockout mice were verified by PCR. **C** Western blotting showed the absence of BAG5 in the testes of $Bag5^{-/-}$ mice at 12-weeks of age. GAPDH loading as control. **D** Number of offspring produced by male $Bag5^{+/+}$ and $Bag5^{-/-}$ mice after mating with wild-type female mice. **E**, **F** The testis size and weight were evaluated in $Bag5^{+/+}$ and $Bag5^{-/-}$ mice, $^{**}P<0.01$. **G** H&E staining of seminiferous tubules and caudal epididymis from $Bag5^{+/+}$ and $Bag5^{-/-}$ mice at 12-weeks of age. **H**, **I** Sperm counts testing in 12-weeks of $Bag5^{+/+}$ and $Bag5^{-/-}$ mice using a sperm counter. $^{***}P<0.001$, Scale bars: 10 μm

BCL2 in testicular tissue slices of $Bag5^{-/-}$ mice was significantly weakened compared to $Bag5^{+/+}$ mice (Fig. 4E). We found *Bcl-2* mRNA and protein amounts were lower in the $Bag5^{-/-}$ group in comparison with the $Bag5^{+/+}$ group (Fig. 4F, G). Consistently, there were more TUNEL-positive germ cells in the $Bag5^{-/-}$ (3.6%) group versus $Bag5^{+/+}$ mice (0.2%) at 12 weeks of age (Fig. 4H, I), which might explain the germ cell loss detected in $Bag5^{-/-}$ mice. The above findings further confirm deficient spermatogenesis in the absence of *Bag5*.

Bag5 deficiency induces the malformation of elongating/elongated spermatids

We next performed morphological analysis of sperm obtained from the tail of the epididymis. Sperm from $Bag5^{-/-}$ mice had severe defective heads. Consistent results were obtained by Pap staining and H&E staining (Fig. 5A, B). To examine the intricacies of DNA organization in the sperm of $Bag5^{+/+}$ and $Bag5^{-/-}$ mice, we used a special sperm nuclear DNA staining kit. Upon employing a specialized sperm head DNA staining technique accompanied by rigorous quantitative analysis, we have discerned a strikingly minimal and notably scattered of DNA condensation within the sperm heads of $Bag5^{-/-}$ mice, when juxtaposed against the prominent condensation observable in the $Bag5^{+/+}$ spermatozoa (Fig. 5C, D). This finding indicates that the absence of BAG5 may lead to disruption of protamine substitution of histones, thereby disrupting the highly organized arrangement of DNA in the sperm head. This hinders the critical compaction required for optimal sperm morphology and functionality, ultimately leading to sperm defects and possible impairment of fertility. To further elucidate the subtle but critical effects of *Bag5* deficiency on sperm integrity, we used both scanning electron microscopy (SEM) and transmission electron microscopy (TEM). In conjunction, SEM images revealed the drastic variations in head shape and contour in $Bag5^{-/-}$ mice, highlighting the structural instability resulting from chromatin mismanagement (Fig. 5E). Complementing the staining results, TEM images provided a high-resolution insight into the ultrastructure of the sperm heads. Notably, in contrast to the densely packed DNA observed in the nuclei of $Bag5^{+/+}$ sperm, the nuclei of $Bag5^{-/-}$ sperm had small, loosely aggregated DNA clusters. Instead of exhibiting the characteristic compact and orderly arrangement of mature sperm, the nuclei of the mutant sperm contained diffuse and disorganized DNA aggregates, demonstrating a clear departure from normal chromatin condensation patterns. We also found partially abnormal 9 + 2 microtubules in some sperm from $Bag5^{-/-}$ mice (Fig. 5F). Jointly, the above findings suggest sperm head chromatin agglutination is affected in $Bag5^{-/-}$ mice.

Deletion of *Bag5* disrupts protamine deposition in sperm

In the final phases of spermiogenesis, protamine deposition on spermatid chromatin occurs, while transition proteins are displaced. To assess the effect of protamine deposition in late spermiogenesis, immunofluorescence staining of TNPs and PRMs was performed. Compared to $Bag5^{+/+}$, the expression and localization of histone H3 were significantly increased in the testes of $Bag5^{-/-}$ mice (Fig. 6A). Signals for TNPs and PRMs decreased in spermatids from $Bag5^{-/-}$ mice (Fig. 6B–E). Western blot analysis of testicular tissue samples also revealed a dramatic reduction in TNPs and PRMs expression in $Bag5^{-/-}$ mice (Fig. 6F–G). Thus, there was an abnormal absence of TNPs and PRMs in sperm, which confirmed an impairment of basic nuclear protein replacement in $Bag5^{-/-}$ mice, with specific deficits of TNPs and subsequent histones in spermatids.

BAG5 interacts with HSPA2 to regulates spermatogenesis

To thoroughly examine how Bag5 deficiency affects testicular gene expression, RNA sequencing was carried out to assess testis samples from 12-week-old $Bag5^{-/-}$ mice. A total of 1229 genes showed a two-fold change in expression in the $Bag5^{-/-}$ group compared to $Bag5^{+/+}$ mice. Of these 1229 differently expressed genes (DEGs), 470 were downregulated in $Bag5^{-/-}$, and *Hspa2* expression decreased significantly (Fig. 7A). The obtained DEGs were submitted to gene ontology analysis, and acrosomal vesicle and 9 + 2 motile cilium, which are associated with spermatogenesis, were shown to be affected (Fig. 7B). We next performed IP-MS analysis to determine proteins with potential interactions with BAG5. MS analysis revealed HSPA2 had the highest abundance among the retrieved proteins (Fig. 7C, D). The online STRING database also indicated an interaction between BAG5 and HSPA2 (Fig. 7E). COIP was also performed to further confirm the interaction between BAG5 and HSPA2. Co-IP was also performed to further confirm that BAG5 interacts with HSPA2 (Fig. 7F). Domain mapping assays suggested BAG5 binds to HSPA2 via multiple

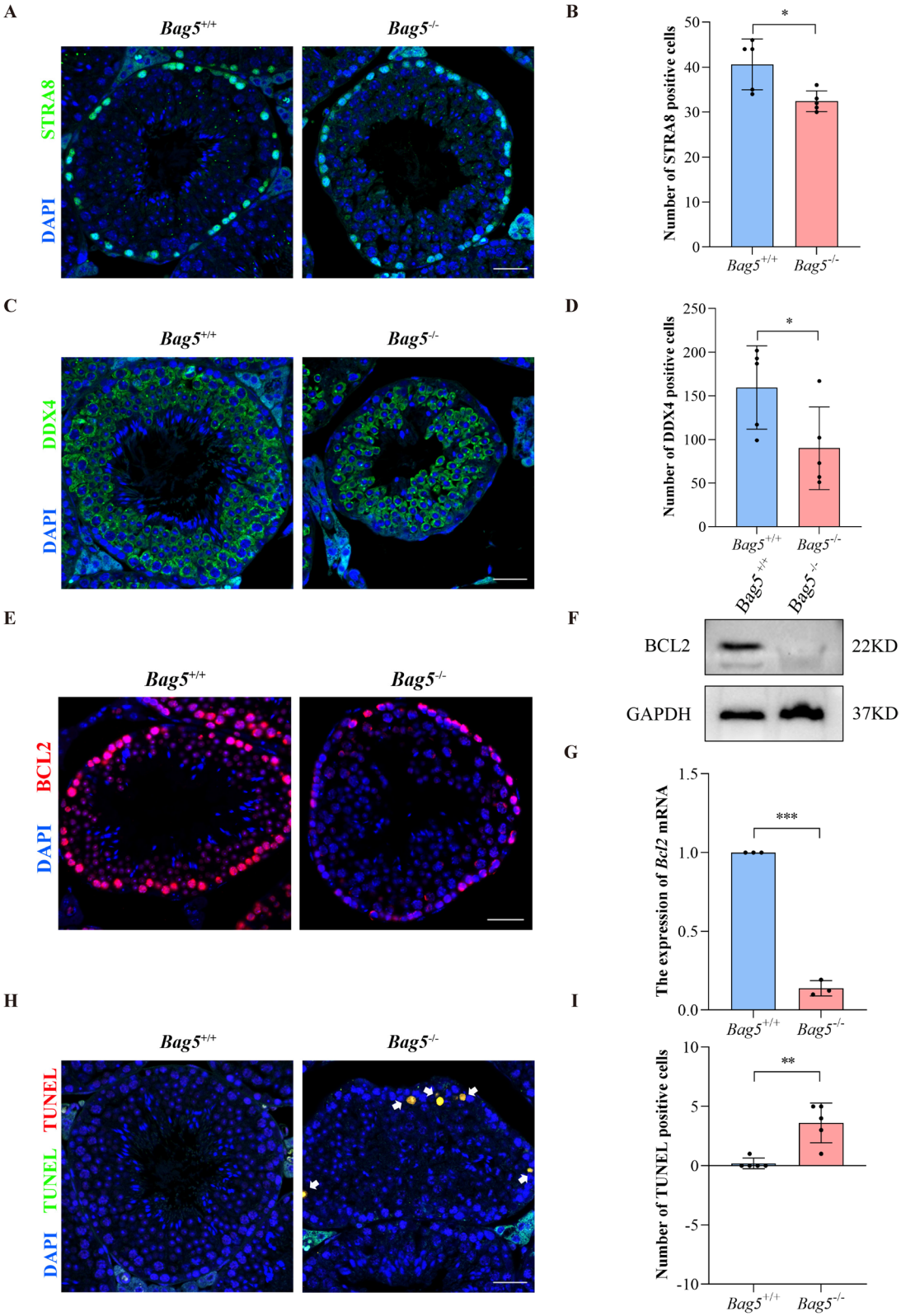

amino acid residues and hydrophobic sequences (Fig. 7G). Meanwhile, testicular HSPA2 was markedly downregulated in *Bag5*$^{-/-}$ mice but not in *Bag5*$^{+/+}$ animals (Fig. 7H). Jointly, the above findings confirmed a specific interaction between BAG5 and HSPA2.

◂**Fig. 4** Deletion of *Bag5* promote apoptosis leads to reduced different types of germ cells. **A** The spermatogonial marker STRA8 was stained in the testes of $Bag5^{+/+}$ and $Bag5^{-/-}$ mice. Scale bars: 50 μm. **B** Statistical analysis of the number of STRA8 positive cells in the testicular tissues of $Bag5^{+/+}$ and $Bag5^{-/-}$ mice. $^{*}P<0.05$. **C** The germ cell marker DDX4 was stained in the testes of $Bag5^{+/+}$ and $Bag5^{-/-}$ mice. Scale bars: 50 μm. **D** Statistical analysis of the number of DDX4 positive cells in the testicular tissues of $Bag5^{+/+}$ and $Bag5^{-/-}$ mice. $^{*}P<0.05$. **E** Localization of anti-apoptotic factor BCL-2 in the testicular tissues of $Bag5^{+/+}$ and $Bag5^{-/-}$ mice. Scale bars: 50 μm. **F**, **G** The expression of BCL-2 mRNA and protein in the testicular tissues of $Bag5^{+/+}$ and $Bag5^{-/-}$ mice. $^{***}P<0.001$. **H** TUNEL staining labeled apoptotic cells in $Bag5^{+/+}$ and $Bag5^{-/-}$ mouse testis. **I** Statistical analysis of the number of TUNEL positive cells in the testicular tissues of $Bag5^{+/+}$ and $Bag5^{-/-}$mice. $^{**}P<0.01$

BAG5 is deficient in samples from patients with nonobstructive azoospermia and oligoasthenospermia

To investigate the importance of BAG5 in human spermatogenesis and fertility, we performed immunofluorescence analyzes on testicular biopsy samples from patients with non-obstructive azoospermia (NOA) and healthy individuals. BAG5 expression was detected in samples from clinically diagnosed patients with nonobstructive azoospermia and oligoasthenospermia. The intensity and distribution of BAG5 staining indicated a significant decrease in both the abundance and location of the protein in testicular tissue samples from patients with non-obstructive azoospermia (Fig. 8A). This observation is consistent with previous findings in mouse models where genetic knockout of *Bag5* resulted in a dramatic decline in germ cells at various developmental stages. *Bag5* mRNA levels were reduced in the NOA testis samples compared to normal controls (Fig. 8B). Before assessing BAG5 expression, we used hematoxylin–eosin staining (H&E) and Papanicolaou staining (Pap) to delineate the structural features that distinguish teratospermic sperm from their normal counterparts. Through meticulous examination, we chose that teratospermic spermatozoa predominantly displayed a range of abnormal heads. In contrast, the normal sperm presented uniform head shapes, straight necks, and symmetrical tails, underscoring the integrity of their structure that promotes reproductive functions (Fig. 8C, D). After morphological characterization, we analyzed BAG5 expression and its localization pattern in teratospermia-affected sperm compared to normal spermatozoa. BAG5 expression was significantly reduced in teratospermic sperm (Fig. 8E), consistent with the phenotype observed in *Bag5*-knockout mice, in which the remaining sperm cells exhibit severe malformation. Overall, *Bag5* deficiency is highly associated with nonobstructive azoospermia and oligoasthenoteratozoospermia, demonstrating consistent and conserved functionality across species, from humans to mice.

BAG5 is a critical regulator that affects multiple steps of spermatogenesis. Bag5 knockout induced apoptosis in male germ cells, disrupted basic nuclear protein deposition on chromatin, and inhibited the expression of TNPs and PRMs, resulting in severe sperm head deformity and a disturbed 9 + 2 microtubule organization. BAG5 interacts with HSPA2, and its deficiency resulted in decreased HSPA2 levels and disturbed spermatogenesis, ultimately causing male infertility (Fig. 8F). That is a snapshot of potential mechanisms controlled by BAG5.

Discussion

The current work assessed transcriptomic data in the GEO database to determine testis-specific genes that participate in spermatogenesis. By database analysis and expression profile verification, BAG5 as a possible regulator of germ cell maturation was retrieved. Using a targeted knockout mouse model, BAG5 was found to be crucial for germ cell development, protamine deposition and chromatin condensation during spermiogenesis. Subsequent mechanistic analysis demonstrated BAG5 functions by interacting with HSPA2, which inhibits germ cell apoptosis and upregulates TNPs and PRMs. Unlike other BAG proteins, BAG5 has been rarely examined for its function, and BAG5's roles in human genetics have not been reported. This study provides novel insights into the physiological role of BAG5 in the regulation of germ cell development.

The current study demonstrated BAG5 plays crucial roles in germ cell survival and maintenance in males. Targeted *Bag5* knockout in mice induced substantial apoptosis in GCs as well as complete male infertility. The first histological abnormality was the reduction in germ cell number as reflected by declined testis weight. Deletion of *Bag5* led to enhanced apoptosis of germ cells, which implicates its important role in anti-apoptosis. Consistently, we observed a decrease in BCL2 expression in $Bag5^{-/-}$ testes, indicating BAG5 may be a BCL-2 associated protein. BCL-2 is crucial for spermatogenesis, regulating germ cell survival [35]. Deficiencies in *Bcl-2*, *Bcl-6* and *Bcl-x* may impair fertility [36–38]. Therefore, BAG5 also plays a role in germ cell development through its anti-apoptotic effects.

Our results show that without BAG5, the normal course of spermiogenesis, especially the condensation step, which is crucial for fitting the paternal genome into the limited volume of the sperm head, is severely impaired. The failure of DNA to compact sufficiently in the absence of BAG5 suggests a disruption in the fine-tuned histone secretion and protamine incorporation processes that are vital for sperm maturation. This disruption not only affects the physical architecture of the sperm nucleus but also potentially impairs its functional capabilities, including the ability to

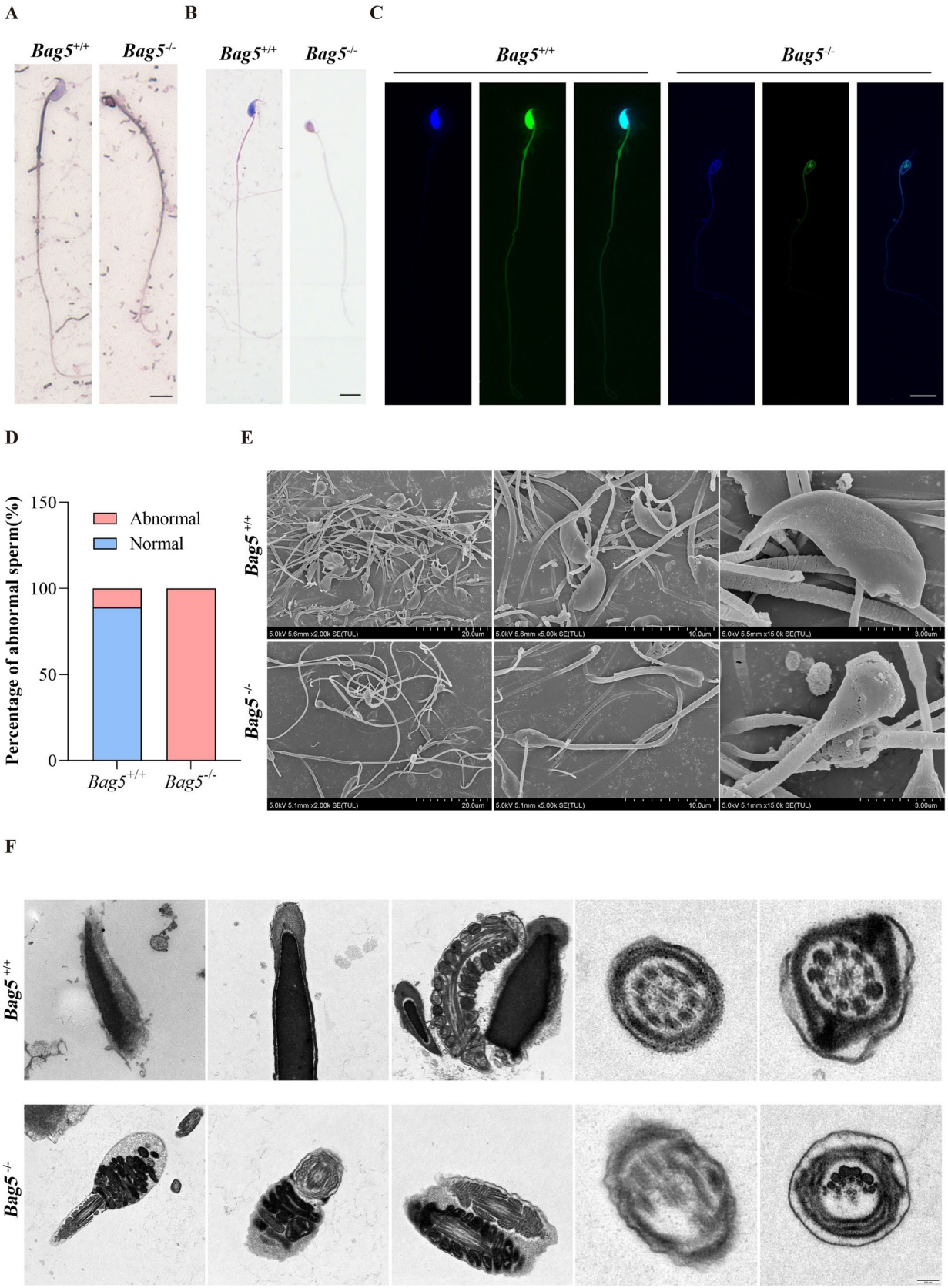
A
B
C
Bag5+/+
Bag5-/-
Bag5+/+
Bag5-/-
Bag5+/+
Bag5-/-
D
E
Percentage of abnormal sperm(%)
150
100
50
0
Abnormal
Normal
Bag5+/+
Bag5-/-
Bag5+/+
Bag5-/-
F
Bag5+/+
Bag5-/-

◂**Fig. 5** *Bag5* deficiency induces defects in sperm count and morphology. **A**, **B** HE and Pap staining analysis of sperm morphology in the epididymal tail of $Bag5^{+/+}$ and $Bag5^{-/-}$ mice. **C** Chromatin condensation in the sperm head of $Bag5^{+/+}$ and $Bag5^{-/-}$mice. **D** Statistical analysis of the percentage of abnormal sperm in $Bag5^{+/+}$ and $Bag5^{-/-}$ mice. **E** SEM of epididymis sperm from $Bag5^{+/+}$ and $Bag5^{-/-}$ mice. Scale bars: 5 μm. **F** TEM analysis of sperm heads and flagella during spermiogenesis in $Bag5^{+/+}$ and $Bag5^{-/-}$ mice. Scale bars: 500 nm

successfully fertilize an egg. The detailed results showed that in the absence of BAG5, the typical high-level DNA condensation in sperm nuclei was significantly disrupted. Histones, which normally occupy the nucleosomes and ensure the proper organization of chromatin, are apparently not removed properly and are replaced by protamines—a characteristic step in spermatogenesis that is responsible for achieving the extreme compaction required for the formation and function of the sperm head is required is essential. The lack of DNA condensation in *Bag5*-deficient sperm highlights the gene's indispensable contribution to the complicated process of chromatin remodeling that occurs en route to germ cell maturation. The second histological anomaly was detected in step-15 spermatids, reflected by severe oligozoospermia, and sperm abnormality. Reduced expression levels of TNPs and PRMs also affect infertility in men [39]. In spermiogenesis, histone replacement with protamines is very important for tight DNA packaging in spermatozoa [40]. Failed translation of TNPs induces histone retention, not even allowing protamine deposition [41]. These findings provide evidence that BAG5 regulates protamine substitution on sperm chromatin.

As depicted above, BAG5 interacts with HSPA2 to affect spermatogenesis. *Bag5* deficiency caused HSPA2 downregulation in the mouse testis. HSPA2 represents a crucial protein in male germ cell development, and its absence suppresses spermatogenic cell development, disrupts meiosis, and induces apoptosis in late stage pachytene spermatocytes [42]. The phenotypic features identified in this work for $Bag5^{-/-}$ mice corroborated these observations. In addition, HSPA2 promotes nuclear translocation of *Tnp1* and *Tnp2*, which are prominent players in DNA packaging in spermatids. Consequently, HSPA2 downregulation results in immature and abnormal sperms in men [43, 44], which was also demonstrated for $Bag5^{-/-}$ mice. This might explain the impaired histone-to-protamine transition and chromatin remodeling detected in $Bag5^{-/-}$ mice. As shown above, *Bag5* deficiency induced HSPA2 downregulation. This work points to BAG5 as an important modulator of HSPA2 in spermatogenesis, highlighting a potential therapeutic target in idiopathic male infertility. Given the limitations of our study, it is important to note that we were unable to accurately determine the exact spatiotemporal distribution of HSPA2 during spermatogenesis due to the limitations imposed by antibody specificity. Despite this limitation, there is a large scientific consensus that HSPA2 plays a crucial role in the complex process of histone substitution with protamine—a fundamental event in sperm formation. This phase, essential for proper chromatin remodeling and compaction, directly influences the structural integrity and motility of mature spermatozoa.

Non-obstructive azoospermia and oligoasthenospermia are two commonly encountered forms of male infertility, with unknown mechanisms. This study found decreased BAG5 expression in both clinical disorders, indicating that BAG5 may represent a prognostic biomarker of male infertility. Considering these findings, further investigation should determine whether *Bag5* mutations and polymorphisms are involved in idiopathic male infertility.

Materials and methods

We applied GSE6969 datasets for screening analysis (https://www.ncbi.nlm.nih.gov/geo/query/acc.cgi?acc=GSE6969). A cross-platform microarray strategy was used to assess the profile of human spermatozoal transcripts from fertile males who had fathered at least one child compared to teratozoospermic individuals. Corresponding data GSM158463-75 (N1-N13, control) vs GSM158476-83 (T1-T8, teratospermia) were used for further analysis. Details of the database used are shown in Supplementary Table 3.

The MHA single cell database

The differential expression of *Bag5* in patients with normal and non-obstructive azoospermia were analyzed in Male Health Atlas single cell sequencing database (MHA: Male Health Atlas; http://malehealthatlas.cn/).

Patients

Testicular biopsies were obtained from 6 infertile men at the Zhongnan Hospital of Wuhan University and submitted to testicular sperm extraction (TESE) to produce

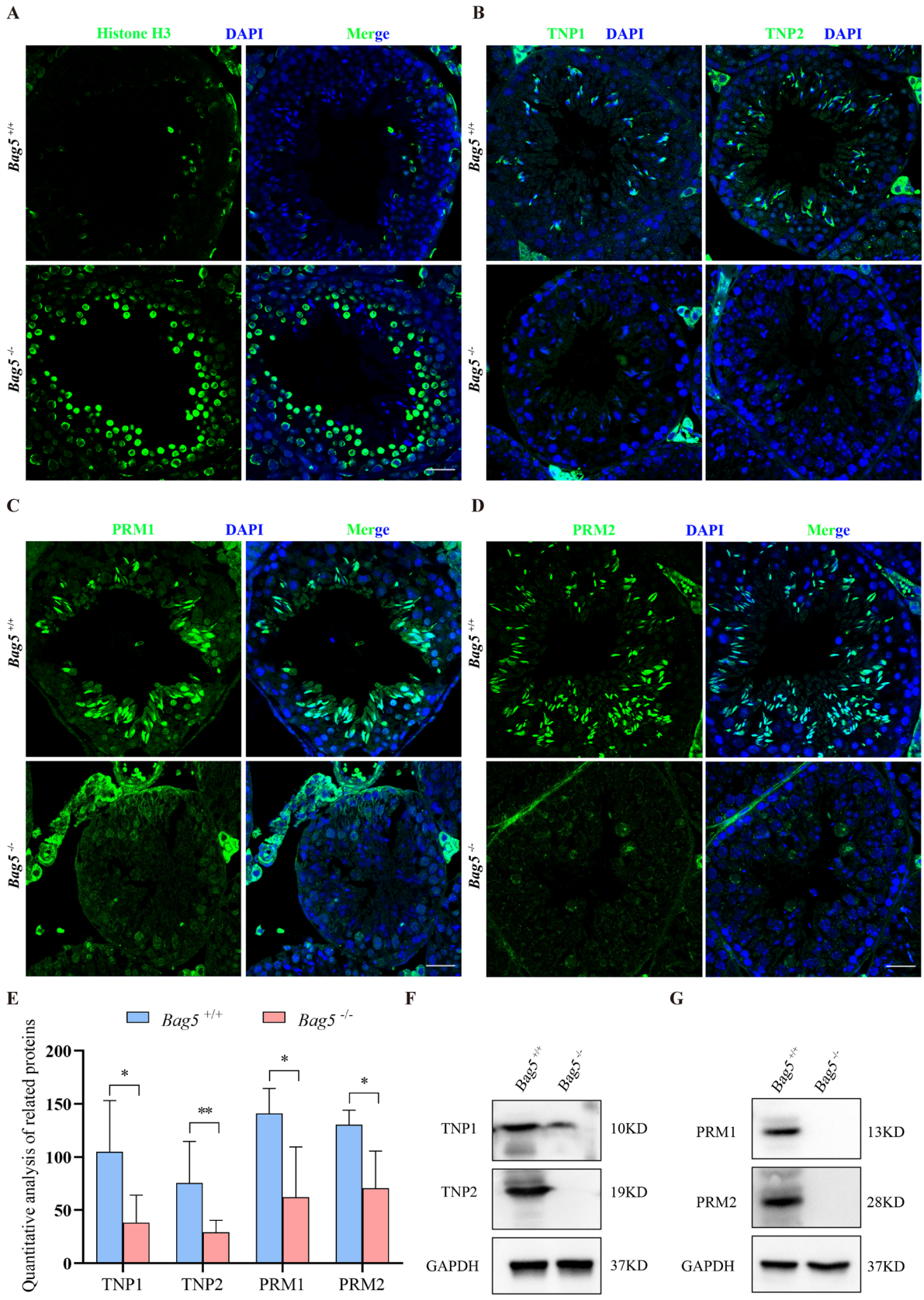
A
Histone H3
DAPI
Merge
Bag5 +/+
Bag5 -/-
B
TNP1
DAPI
TNP2
DAPI
C
PRM1
DAPI
Merge
D
PRM2
DAPI
Merge
E
Bag5 +/+
Bag5 -/-
Quantitative analysis of related proteins
200
150
100
50
0
*
**
*
*
TNP1
TNP2
PRM1
PRM2
F
Bag5 +/+
Bag5 -/-
TNP1
10KD
TNP2
19KD
GAPDH
37KD
G
Bag5 +/+
Bag5 -/-
PRM1
13KD
PRM2
28KD
GAPDH
37KD

◂**Fig. 6** *Bag5* deficiency leads to reduced protamine deposition in sperm. **A** Immunofluorescence analysis of histone H3 localization in testicular tissues from $Bag5^{+/+}$ and $Bag5^{-/-}$ mice. **B** Immunofluorescence analysis of TNPs localization in testicular tissues of $Bag5^{+/+}$ and $Bag5^{-/-}$ mice. **C** Immunofluorescence analysis of PRM1 localization in testicular tissues of $Bag5^{+/+}$ and $Bag5^{-/-}$ mice. **D** Immunofluorescence analysis of PRM2 localization in testicular tissues from $Bag5^{+/+}$ and $Bag5^{-/-}$ mice. **E** Quantitative results of Figure A-D. $^{**}P<0.01$, $^{*}P<0.05$. F-G. Western blot analysis of TNPs and PRMs expression in testicular tissues of $Bag5^{+/+}$ and $Bag5^{-/-}$ mice

spermatozoa for intracytoplasmic sperm injection (ICSI). Totally 6 healthy testis and sperm samples from donors served as controls. The sperm samples were classified as normozoospermia and oligoasthenospermia according to the WHO. This study had approval from the Institutional Ethics Committee (NO. 2022013 K), and each participant provided signed informed consent before the collection of tissue samples.

Mice

$Bag5^{-/-}$ mice were obtained via heterozygous breeding performed by Cyagen Biosciences. PCR and Sanger sequencing were performed to confirm the mouse genotype. This study used 12-week-old animals and was approved by the Animal Experimentation Ethics Committee of the Fifth Affiliated Hospital of Sun Yat-sen University (NO. 00234). Details of the used primers are shown in Supplementary Table 1.

Histological analysis and immunostaining

Testes extracted from 12-week-old animals underwent fixation with Bouin's solution. 5-μm sections were employed for H&E staining and Pap. In immunofluorescence, frozen testis sections underwent a 4-min incubation with 1% SDS for antigen retrieval. Cauda epididymis sections underwent a 30-min incubation with 10 mM dithiothreitol with heating in a microwave for antigen retrieval. After successive incubations with primary (4 ℃, overnight) and secondary antibodies (Supplementary Table 2), DAPI counterstaining was carried out. The results of immunofluorescence staining were quantitatively analyzed by Photoshop identification of positive signals in testicular tissue sections of $Bag5^{+/+}$ and $Bag5^{-/-}$ mice.

Fertility test

To assess fertility in $Bag5^{-/-}$ male mice, 8-week-old animals were employed, mating $Bag5^{-/-}$ males with wild-type C57BL/6 females. Cages were checked at 1–2 day intervals for newly born pups. The assay was stopped with female mice failing to produce pups for 6 months.

Sperm count

Caudal epididymis samples were submitted to dissection, followed by immersion in 1 ml of M2 medium. The samples underwent mincing to allow sperm cells into the medium by swimming for 10 min at 37 °C. After dilution with PBS, the samples were examined using an SCA automatic animal sperm analyzer (SCA-V-P02) at the School of Oceanography, Sun Yat-sen University (https://marine.sysu.edu.cn/) to determine sperm.

TUNEL assay

Mouse testis samples underwent fixation with Bouin solution (24 h), followed by transfer into 70% ethanol. After dehydration with graded ethanol and paraffin embedding, tissue sections were obtained. Apoptosis was assessed with a Roche cell apoptosis kit as directed by the manufacturer. Apoptotic cell number/tubule was the ratio of total number of TUNEL-positive germ cells by the total number of seminiferous tubules.

RT-PCR

Testis samples were obtained from $Bag5^{+/+}$ and $Bag5^{-/-}$ mice. Total RNA extraction from cell and testis samples used TRIZOL. The SuperScript First-Strand kit was employed for reverse transcription as directed by the manufacturer. Table S1 lists all primers used for RT-PCR.

Scanning electron microscopy

Sperm samples underwent a 2-h fixation with 2.5% glutaraldehyde at 4 °C and placement on poly-L-lysine-treated coverslips. After washing with distilled water, dehydration with graded ethyl alcohol (successively 50%, 70%, 80%, 90% and 100%) and drying with a Quorum K850 Critical Point Dryer were carried out. The specimens underwent coating with gold particles before imaging on an S-3400 N SEM.

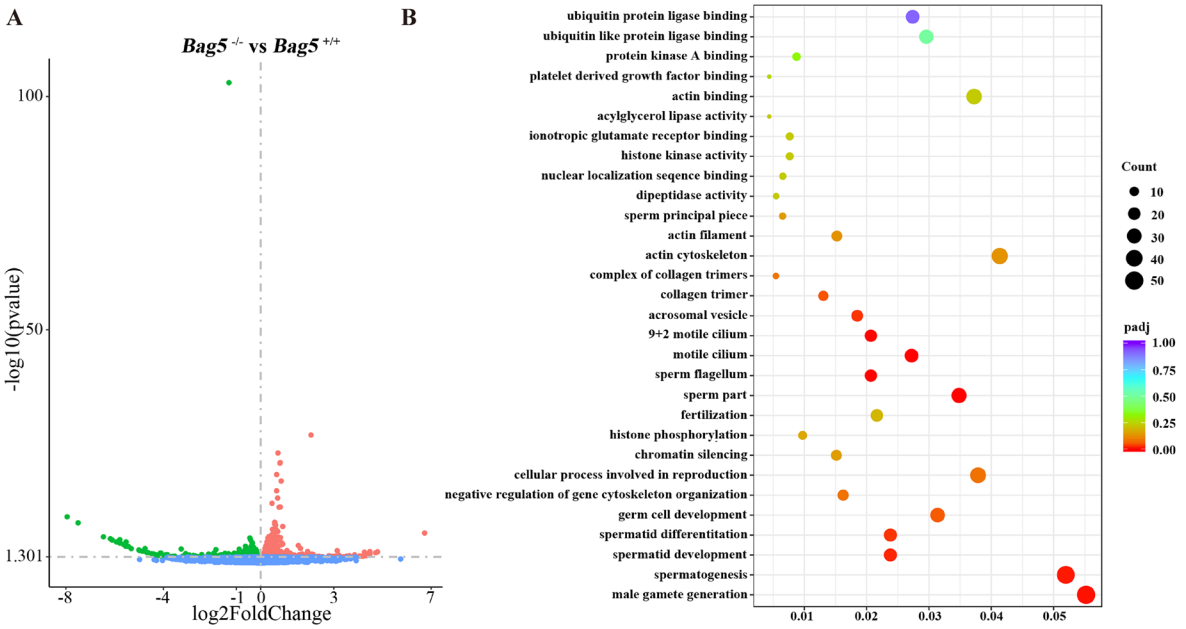

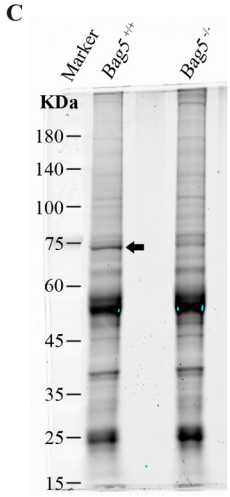

D

Protein	Description	KD
HSPA2	Heat shock-related 70 kDa protein 2	70
RBM14	RNA-binding protein 14	66
HNRNPK	Heterogeneous nuclear ribonucleoprotein K	51
HSPA8	Heat shock cognate 71 kDa protein	71
HNRNPL	Heterogeneous nuclear ribonucleoprotein L	64
HSPA5	78 kDa glucose-regulated protein	78
KRT10	Keratin, type I cytoskeletal 10	57
HNRNPU	Heterogeneous nuclear ribonucleoprotein U	88
VCP	Transitional endoplasmic reticulum ATPase	80
DDX4	RNA helicase	79

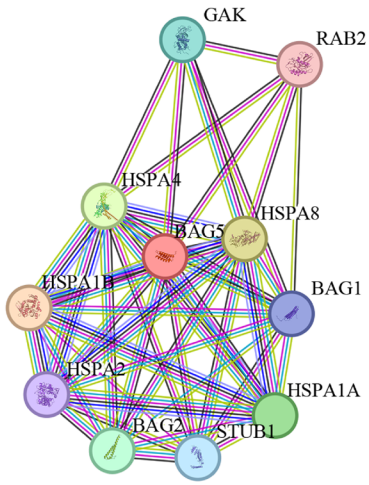

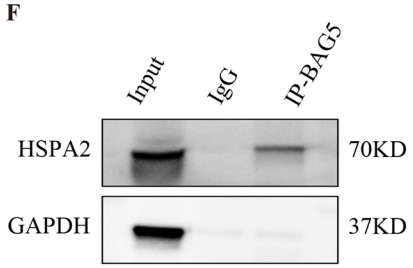

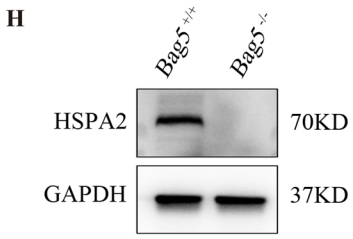

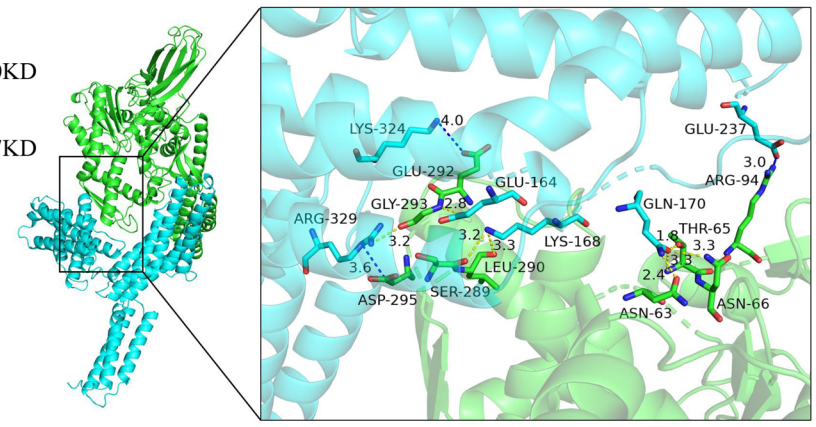

◂**Fig. 7** BAG5 interacts with HSPA2 to maintenance spermatogenesis. **A** RNA seq analysis of differentially expressed genes in the testicular tissues of $Bag5^{+/+}$ and $Bag5^{-/-}$ mice. **B** GO analysis of differentially expressed genes in the testicular tissues of $Bag5^{+/+}$ and $Bag5^{-/-}$ mice. **C**, **D** IP-MS analysis of differential proteins in testicular tissues of $Bag5^{+/+}$ and $Bag5^{-/-}$ mice. **E** The STRING database analyzed the interacting proteins of BAG5. **F** CO-IP confirms that BAG5 interacts with HSPA2. **G** Molecular docking verification of binding activity between BAG5 and HSPA2. **H** Western blot analysis of HSPA2 expression in testicular tissues of $Bag5^{+/+}$ and $Bag5^{-/-}$ mice, GAPDH loading as control

Transmission electron microscopy evaluation

Fresh mouse sperm specimens underwent fixation with 2.5% glutaraldehyde. They were dehydrated and submitted to Epon 812 embedding. Ultrathin sections underwent staining with uranyl acetate and lead citrate for imaging with a TEM at 80 kV.

RNA sequencing

Total RNA extraction from testis samples from 12-week-old $Bag5^{+/+}$ and $Bag5^{-/-}$ mice employed an RNA extraction kit containing DNase I. In our sample selection and processing, equal volumes and weights of decapsulated mouse testis tissue, stripped of tunica albuginea, were used for RNA extraction. Post-RNA extraction, quantitative homogenization was applied to ensure consistency across samples before proceeding with further analyses. RNA-seq was performed by Novogene, using routine methods. An Illumina HiSeq 4000 Genome Analyzer was utilized for sequencing. Standard bioinformatics was conducted by Novogene.

Immunoprecipitation

To assess BAG5's interaction with HSPA2, testis lysates were added to protein G beads for overnight incubation at 4 ℃. Then, 4 μg rabbit anti-BAG5 antibodies or normal rabbit IgG were added for overnight incubation at 4 ℃. Next, protein A beads were supplemented for a 6-h incubation at 4 ℃. The target proteins pulled by BAG5 in the lytic fluid of $Bag5^{+/+}$ and $Bag5^{-/-}$ testicular tissue were ruby stained, and various bands were identified by mass spectrometry. Immunoblot was used to examine the eluted proteins with anti-HSPA2 antibodies. The IP experiment was repeated 3 times and the mass spectrometry was repeated 2 times.

Immunoblot

Protein separation used SDS-PAGE, and the protein bands were electro-transferred onto polyvinylidene difluoride membranes. After a 2-h blocking with 5% nonfat milk at ambient, overnight incubation was carried out at 4 °C with various primary antibodies (Table S2). Subsequently, appropriate secondary antibodies were added for a 2-h incubation at ambient. The ECL Western blot kit was utilized for development as directed by the manufacturer. Details of the antibodies used are shown in Supplementary Table 2.

Statistical analysis

Quantitative variables are Mean ± SEM. Unpaired Student's t-test was performed for comparisons, with $P < 0.05$ indicating statistical significance. At least 3 independent assays were performed in triplicate. Data analysis used GraphPad.

Conflict of interest

The authors have no relevant financial or non-financial interests to disclose.

Ethical approval and consent to participate

The sperm samples were classified as normozoospermia and oligoasthenospermia according to the WHO. This study had approval from the Institutional Ethics Committee (NO. 2022013 K). Participants who were included in the study provided informed consent. Th animals' experiment had approval from The Fifth Affiliated Hospital of Sun Yat-sen

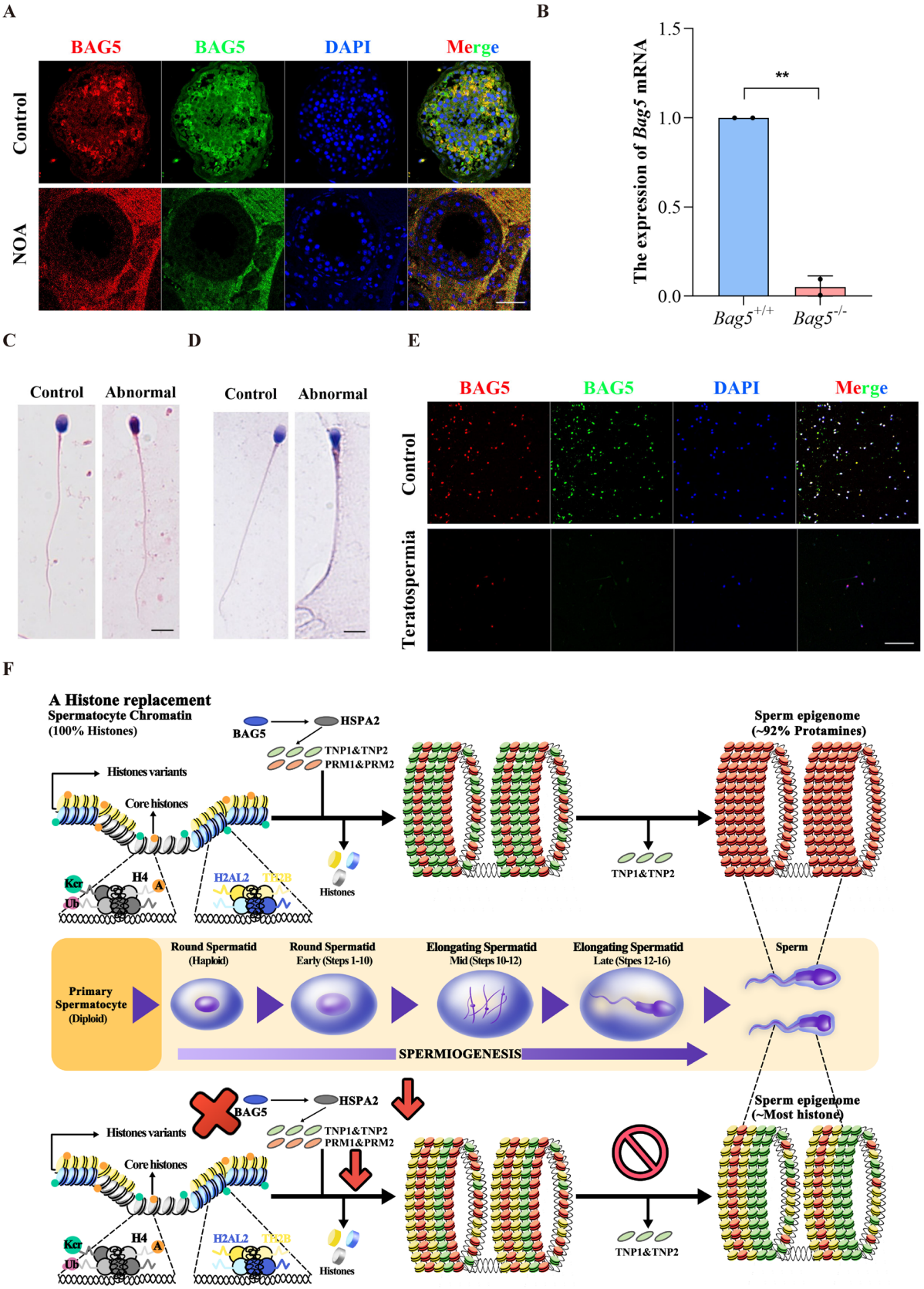
A
BAG5
BAG5
DAPI
Merge
Control
NOA
B
The expression of Bag5 mRNA
1.5
1.0
0.5
0.0
**
Bag5+/+
Bag5-/-
C
Control
Abnormal
D
Control
Abnormal
E
BAG5
BAG5
DAPI
Merge
Control
Teratospermia
F
A Histone replacement
Spermatocyte Chromatin
(100% Histones)
BAG5
HSPA2
TNP1&TNP2
PRM1&PRM2
Histones variants
Core histones
Kcr
Ub
H4
A
H2AL2
TH2B
Histones
TNP1&TNP2
Sperm epigenome
(~92% Protamines)
Primary
Spermatocyte
(Diploid)
Round Spermatid
(Haploid)
Round Spermatid
Early (Steps 1-10)
Elongating Spermatid
Mid (Steps 10-12)
Elongating Spermatid
Late (Stpes 12-16)
Sperm
SPERMIOGENESIS
BAG5
HSPA2
TNP1&TNP2
PRM1&PRM2
Histones variants
Core histones
Kcr
Ub
H4
A
H2AL2
TH2B
Histones
TNP1&TNP2
Sperm epigenome
(~Most histone)

◂**Fig. 8** BAG5 is downregulated in patients with nonobstructive azoospermia and oligonasthenospermia. **A** Localization of BAG5 in nonobstructive azoospermia and normal healthy male testicular tissue (Red: BAG5-mouse Cat No. SC-390832, Green: BAG5-Rabbit Cat No. 26628–1-AP, Blue: DAPI). **B** Expression of *Bag5* mRNA in testicular tissues of non-obstructive azoospermia and normal healthy males. **C** Morphological analysis of Pap staining in oligoasthenozoospermia and normal healthy male sperm. **D** Morphological analysis of HE staining in oligoasthenozoospermia and normal healthy male sperm. **E** Localization of BAG5 in oligoasthenozoospermia and normal healthy male sperm (Red: BAG5-mouse Cat No. sc-390832, Green: BAG5-Rabbit Cat No. 26628–1-AP, Blue: DAPI). **F** Schematic illustration of the mechanisms that are possibly dependent on the presence of the BAG5

University Animal Experimentation Ethics Committee (NO. 00234).

Consent for publication

The final version of the article for submission had been read and approved by all co-authors. All authors agreed to its submission for publication and signed informed consent about the publication of data and images.

Supplementary Information The online version contains supplementary material available at https://doi.org/10.1007/s00018-025-05591-2.

Acknowledgements We would like to acknowledge the patient and his family members for participating in our research. The author thanks all members who helped with the research. We thank MedSci for its linguistic assistance during the preparation of this manuscript. The authors thank the editors and reviewers for their significant contributions during the revision period.

Author contribution YM.C. and L.W. were involved in the conception and design of the study. YM.C., SN.W., ZH.Q., WW.L., LY.L., ZX. W and J.L. performed experiments and data analysis. All authors read and contributed to previous versions of the manuscript. All authors approved the final article for submission.

Funding This project was supported by grants from the National Natural Science Foundation of China (Grant No. 82301804), the China postdoctoral science foundation (Grant No. 2023M734014).

Data availability In our study, all data and materials are available from the corresponding author on reasonable request.

References

1. Chen Y, Zheng Y, Gao Y, Lin Z, Yang S, Wang T, Wang Q, Xie N, Hua R, Liu M, Sha J, Griswold MD, Li J, Tang F, Tong MH (2018) Single-cell RNA-seq uncovers dynamic processes and critical regulators in mouse spermatogenesis. Cell Res 28(9):879–896
2. Murat F, Mbengue N, Winge SB, Trefzer T, Leushkin E, Sepp M, Cardoso-Moreira M, Schmidt J, Schneider C, Mossinger K, Bruning T, Lamanna F, Belles MR, Conrad C, Kondova I, Bontrop R, Behr R, Khaitovich P, Paabo S, Marques-Bonet T, Grutzner F, Almstrup K, Schierup MH, Kaessmann H (2023) The molecular evolution of spermatogenesis across mammals. Nature 613(7943):308–316
3. Kopania EEK, Larson EL, Callahan C, Keeble S, Good JM (2022) Molecular evolution across mouse spermatogenesis. Mol Biol Evol 39(2):msac023
4. Flury V, Reveron-Gomez N, Alcaraz N, Stewart-Morgan KR, Wenger A, Klose RJ, Groth A (2023) Recycling of modified H2A–H2B provides short-term memory of chromatin states. Cell 186(5):1050-1065 e19
5. Cao Y, Sun Q, Chen Z, Lu J, Geng T, Ma L, Zhang Y (2022) CDKN2AIP is critical for spermiogenesis and germ cell development. Cell Biosci 12(1):136
6. Hernandez DJ, Kiesewetter KN, Almeida BK, Revillini D, Afkhami ME (2023) Multidimensional specialization and generalization are pervasive in soil prokaryotes. Nat Ecol Evol 7(9):1408–1418
7. Meng C, Liao J, Zhao D, Huang H, Qin J, Lee TL, Chen D, Chan WY, Xia Y (2019) L3MBTL2 regulates chromatin remodeling during spermatogenesis. Cell Death Differ 26(11):2194–2207
8. Li C, Shen C, Xiong W, Ge H, Shen Y, Chi J, Zhang H, Tang L, Lu S, Wang J, Fei J, Wang Z (2024) Spem2, a novel testis-enriched gene, is required for spermiogenesis and fertilization in mice. Cell Mol Life Sci 81(1):108
9. Li W, Wu J, Kim SY, Zhao M, Hearn SA, Zhang MQ, Meistrich ML, Mills AA (2014) Chd5 orchestrates chromatin remodelling during sperm development. Nat Commun 5:3812
10. Moritz L, Schon SB, Rabbani M, Sheng Y, Agrawal R, Glass-Klaiber J, Sultan C, Camarillo JM, Clements J, Baldwin MR, Diehl AG, Boyle AP, O'Brien PJ, Ragunathan K, Hu YC, Kelleher NL, Nandakumar J, Li JZ, Orwig KE, Redding S, Hammoud SS (2023) Sperm chromatin structure and reproductive fitness are altered by substitution of a single amino acid in mouse protamine 1. Nat Struct Mol Biol 30(8):1077–1091
11. Amjad S, Mushtaq S, Rehman R, Munir A, Zahid N, Siddique PQR (2021) Protamine 1/protamine 2 mRNA ratio in nonobstructive azoospermic patients. Andrologia 53(3):e13936
12. Braun RE (2001) Packaging paternal chromosomes with protamine. Nat Genet 28(1):10–12
13. Gibson BA, Blaukopf C, Lou T, Chen L, Doolittle LK, Finkelstein I, Narlikar GJ, Gerlich DW, Rosen MK (2023) In diverse conditions, intrinsic chromatin condensates have liquid-like material properties. Proc Natl Acad Sci U S A 120(18):e2218085120
14. Phillips BT, Williams JG, Atchley DT, Xu X, Li JL, Adams AL, Johnson KL, Hall TMT (2019) Mass spectrometric identification of candidate RNA-binding proteins associated with transition nuclear protein mRNA in the mouse testis. Sci Rep 9(1):13618
15. Merges GE, Meier J, Schneider S, Kruse A, Frobius AC, Kirfel G, Steger K, Arevalo L, Schorle H (2022) Loss of Prm1 leads to

defective chromatin protamination, impaired PRM2 processing, reduced sperm motility and subfertility in male mice. Development. https://doi.org/10.1242/dev.200330
16. Fang Q, Chen XL, Zhang L, Li YB, Sun TZ, Yang CX, Chang JF, Yang XM, Sun F (2021) The essential roles of Mps1 in spermatogenesis and fertility in mice. Cell Death Dis 12(6):531
17. Geister KA, Brinkmeier ML, Cheung LY, Wendt J, Oatley MJ, Burgess DL, Kozloff KM, Cavalcoli JD, Oatley JM, Camper SA (2015) LINE-1 mediated insertion into Poc1a (protein of centriole 1 A) causes growth insufficiency and male infertility in mice. PLoS Genet 11(10):e1005569
18. Zhou H, Li J, Liu X, Wei X, He Z, Hu L, Wang J, Duan M, Xie G, Wang J, Wang L (2021) The Divergent roles of the rice bcl-2 associated athanogene (BAG) genes in plant development and environmental responses. Plants (Basel) 10(10):2169
19. Bruchmann A, Roller C, Walther TV, Schafer G, Lehmusvaara S, Visakorpi T, Klocker H, Cato AC, Maddalo D (2013) Bcl-2 associated athanogene 5 (Bag5) is overexpressed in prostate cancer and inhibits ER-stress induced apoptosis. BMC Cancer 13:96
20. Tedesco B, Vendredy L, Timmerman V, Poletti A (2023) The chaperone-assisted selective autophagy complex dynamics and dysfunctions. Autophagy 19(6):1619–1641
21. Chen Y, Yang LN, Cheng L, Tu S, Guo SJ, Le HY, Xiong Q, Mo R, Li CY, Jeong JS, Jiang L, Blackshaw S, Bi LJ, Zhu H, Tao SC, Ge F (2013) Bcl2-associated athanogene 3 interactome analysis reveals a new role in modulating proteasome activity. Mol Cell Proteomics 12(10):2804–2819
22. Song H, Chen D, Bai R, Feng Y, Wu S, Wang T, Xia X, Li J, Miao YL, Zuo B, Li F (2022) BCL2-associated athanogene 6 exon24 contributes to testosterone synthesis and male fertility in mammals. Cell Prolif 55(7):e13281
23. Yang J, Grafton F, Ranjbarvaziri S, Budan A, Farshidfar F, Cho M, Xu E, Ho J, Maddah M, Loewke KE, Medina J, Sperandio D, Patel S, Hoey T, Mandegar MA (2022) Phenotypic screening with deep learning identifies HDAC6 inhibitors as cardioprotective in a BAG3 mouse model of dilated cardiomyopathy. Sci Transl Med 14(652):eabl5654
24. Bromfield EG, Aitken RJ, McLaughlin EA, Nixon B (2017) Proteolytic degradation of heat shock protein A2 occurs in response to oxidative stress in male germ cells of the mouse. Mol Hum Reprod 23(2):91–105
25. Zhao B, Qin X, Fu R, Yang M, Hu X, Zhao S, Cui Y, Guo Q, Zhou W (2024) Supramolecular nanodrug targeting CDK4/6 overcomes BAG1 mediated cisplatin resistance in oral squamous cell carcinoma. J Control Release 368:623–636
26. Carrettiero DC, Almeida MC, Longhini AP, Rauch JN, Han D, Zhang X, Najafi S, Gestwicki JE, Kosik KS (2022) Stress routes clients to the proteasome via a BAG2 ubiquitin-independent degradation condensate. Nat Commun 13(1):3074
27. Hu F, Yu Y, Chen JS, Hu H, Scheet P, Huff CD (2021) Integrated case-control and somatic-germline interaction analyses of soft-tissue sarcoma. J Med Genet 58(3):145–153
28. Bromfield E, Aitken RJ, Nixon B (2015) Novel characterization of the HSPA2-stabilizing protein BAG6 in human spermatozoa. Mol Hum Reprod 21(10):755–769
29. Sojka DR, Abramowicz A, Adamiec-Organisciok M, Karnas E, Mielanczyk L, Kania D, Blamek S, Telka E, Scieglinska D (2023) Heat shock protein A2 is a novel extracellular vesicle-associated protein. Sci Rep 13(1):4734
30. Horste EL, Fansler MM, Cai T, Chen X, Mitschka S, Zhen G, Lee FCY, Ule J, Mayr C (2023) Subcytoplasmic location of translation controls protein output. Mol Cell 83(24):4509-4523 e11
31. Gomez-Torres MJ, Huerta-Retamal N, Saez-Espinosa P, Robles-Gomez L, Aviles M, Aizpurua J (2023) Molecular chaperone HSPA2 distribution during hyaluronic acid selection in human sperm. Reprod Sci 30(4):1176–1185
32. Kumaresan A, Sinha MK, Paul N, Nag P, Ebenezer Samuel King JP, Kumar R, Datta TK (2023) Establishment of a repertoire of fertility associated sperm proteins and their differential abundance in buffalo bulls (Bubalus bubalis) with contrasting fertility. Sci Rep 13(1):2272
33. Redgrove KA, Nixon B, Baker MA, Hetherington L, Baker G, Liu DY, Aitken RJ (2012) The molecular chaperone HSPA2 plays a key role in regulating the expression of sperm surface receptors that mediate sperm-egg recognition. PLoS ONE 7(11):e50851
34. Kahrl AF, Snook RR, Fitzpatrick JL (2021) Fertilization mode drives sperm length evolution across the animal tree of life. Nat Ecol Evol 5(8):1153–1164
35. Lindenboim L, Zohar H, Gundersen GG, Worman HJ, Stein R (2024) LINC complex protein nesprin-2 has pro-apoptotic activity via Bcl-2 family proteins. Cell Death Discov 10(1):29
36. Li X, Yi H, Wang H (2018) Sulphur dioxide and arsenic affect male reproduction via interfering with spermatogenesis in mice. Ecotoxicol Environ Saf 165:164–173
37. Kwon J, Mochida K, Wang YL, Sekiguchi S, Sankai T, Aoki S, Ogura A, Yoshikawa Y, Wada K (2005) Ubiquitin C-terminal hydrolase L-1 is essential for the early apoptotic wave of germinal cells and for sperm quality control during spermatogenesis. Biol Reprod 73(1):29–35
38. Klimczak AM, Herlihy NS, Scott CS, Hanson BM, Kim JG, Titus S, Seli E, Scott RT Jr (2022) B-cell lymphoma 6 expression is not associated with live birth in a normal responder in vitro fertilization population. Fertil Steril 117(2):351–358
39. Miyagawa Y, Nishimura H, Tsujimura A, Matsuoka Y, Matsumiya K, Okuyama A, Nishimune Y, Tanaka H (2005) Single-nucleotide polymorphisms and mutation analyses of the TNP1 and TNP2 genes of fertile and infertile human male populations. J Androl 26(6):779–786
40. Huang C, Gong H, Mu B, Lan X, Yang C, Tan J, Liu W, Zou Y, Li L, Feng B, He X, Luo Q, Chen Z (2022) BAF-L modulates histone-to-protamine transition during spermiogenesis. Int J Mol Sci 23(4):1985
41. Yoshida K, Muratani M, Araki H, Miura F, Suzuki T, Dohmae N, Katou Y, Shirahige K, Ito T, Ishii S (2018) Mapping of histone-binding sites in histone replacement-completed spermatozoa. Nat Commun 9(1):3885
42. Bromfield EG, McLaughlin EA, Aitken RJ, Nixon B (2016) Heat Shock Protein member A2 forms a stable complex with angiotensin converting enzyme and protein disulfide isomerase A6 in human spermatozoa. Mol Hum Reprod 22(2):93–109
43. Govin J, Caron C, Escoffier E, Ferro M, Kuhn L, Rousseaux S, Eddy EM, Garin J, Khochbin S (2006) Post-meiotic shifts in HSPA2/HSP70.2 chaperone activity during mouse spermatogenesis. J Biol Chem 281(49):37888–92
44. Yin Y, Cao S, Fu H, Fan X, Xiong J, Huang Q, Liu Y, Xie K, Meng TG, Liu Y, Tang D, Yang T, Dong B, Qi S, Nie L, Zhang H, Hu H, Xu W, Li F, Dai L, Sun QY, Li Z (2020) A noncanonical role of NOD-like receptor NLRP14 in PGCLC differentiation and spermatogenesis. Proc Natl Acad Sci U S A 117(36):22237–22248